

Confirmation of production of element 110 by the $^{208}\text{Pb}(^{64}\text{Ni},n)$ reaction

T. N. Ginter,^{1,*} K. E. Gregorich,¹ W. Loveland,² D. M. Lee,¹ U. W. Kirbach,¹ R. Sudowe,¹ C. M. Folden III,^{1,3} J. B. Patin,^{1,3} N. Seward,⁴ P. A. Wilk,¹ P. M. Zielinski,^{1,3} K. Aleklett,⁵ R. Eichler,⁶ H. Nitsche,^{1,3} and D. C. Hoffman^{1,3}

¹Nuclear Science Division, Lawrence Berkeley National Laboratory, Berkeley, California 94720, USA

²Department of Chemistry, Oregon State University, Corvallis, Oregon 97331, USA

³Department of Chemistry, University of California, Berkeley, California 94720, USA

⁴Physics Department, University of Surrey, Surrey, United Kingdom

⁵Uppsala University, Uppsala, Sweden

⁶Paul Scherrer Institute, Villigen PSI, Switzerland

(Received 6 February 2003; published 27 June 2003; corrected 9 July 2003)

We report the experimental confirmation of the production of element 110. In the bombardment of a ^{208}Pb target with a 309-MeV ^{64}Ni beam, we have observed two chains of time- and position-correlated events. Each chain consisted of the implantation of an evaporation residue followed by the emission of α particles. We attribute these two chains to the decay of $^{271}110$ produced with a cross section of $8.3_{-5.3}^{+11}$ pb.

DOI: 10.1103/PhysRevC.67.064609

PACS number(s): 25.70.Jj, 25.70.Gh, 27.90.+b

The synthesis of element 110 has been reported at three laboratories: the Lawrence Berkeley National Laboratory (LBNL) in the United States [1], the Gesellschaft für Schwerionenforschung (GSI) in Germany [2–6], and the Joint Institute for Nuclear Research (JINR) in Russia [7–9]. Table I provides a summary of the isotopes observed, the production mechanism, their observed decay modes, and references. None of these observations confirm the others since they all involved different isotopes. (In the case of $^{273}110$, which was reported both at the JINR and the GSI, the α decays observed did not have matching energies and lifetimes; although “not in contradiction” [3], these results do not confirm each other.) Furthermore, none of the work has been confirmed independently in an experimental setup not used in the original work; such verification is essential for establishing the credibility of the results because of the challenging nature of the experiments.

In 1998, Hofmann produced $^{271}110$ in the $^{208}\text{Pb}(^{64}\text{Ni},n)$ reaction [5]. They observed a total of nine events—two at a beam energy of 311.7 MeV, six at 313.0 MeV, and one at 315.5 MeV. This nuclide decays by α emission ($E_\alpha = 10.74, 10.68$ MeV, $t_{1/2} = 1.1_{-3}^{+6}$ ms and $E_\alpha = 10.71$ MeV, $t_{1/2} = 0.06_{-0.03}^{+0.27}$ s [10]) to ^{267}Hs [11]. Here we report the successful repetition of the synthesis of $^{271}110$ using the same reaction [12].

We performed this study using the Berkeley gas-filled separator (BGS) [13] at the LBNL 88-inch cyclotron facility. The cyclotron delivered the $^{64}\text{Ni}^{14+}$ beam at an average current of ~ 250 particle nA and at energies of 312.5, 315, and 317.5 MeV. Measurements of the beam energy reproducibility give a standard deviation of 0.2% [14].

The ^{208}Pb target was located at the front of the BGS, about 5 mm downstream from the separator’s 40- $\mu\text{g}/\text{cm}^2$ carbon entrance window. The target consisted of nine arc-

shaped segments, each with a 500- $\mu\text{g}/\text{cm}^2$ thick lead layer sandwiched between layers of carbon with thicknesses of 40 $\mu\text{g}/\text{cm}^2$ (facing the beam) and 2 $\mu\text{g}/\text{cm}^2$. These segments were mounted around the periphery of a 14-inch diameter wheel which was rotated to minimize thermal stress on the target from beam heating. The beam energies at the center of the target were 306.7, 309.2, and 312.8 MeV [15]; the energy thickness of the target was 6 MeV for all three energies. Two silicon *p-i-n* detectors (mounted at ± 27 degrees with respect to the incident beam) monitored the product of beam intensity and target thickness by detecting beam particles that were elastically scattered from the target.

The BGS spatially separated the recoiling fusion-evaporation residues (EVR’s, $E \sim 70$ MeV) in flight from both beam particles and transfer reaction products on the basis of their differing magnetic rigidities within the separator’s 0.88-torr helium atmosphere. The magnetic rigidity $B\rho$ of the $^{271}110$ EVR’s was estimated to be 2.1 T m [16]. We extrapolated the BGS magnetic field setting used for the $^{271}110$ reaction from the setting that centered the EVR distribution (with an estimated $B\rho$ of 1.47 T m) from the reaction of ^{64}Ni at 309 MeV on ^{120}Sn .

At the BGS focal plane, the EVR’s were deposited into a

TABLE I. Summary of previously observed element 110 isotopes.

Isotope	Production mechanism	Decay mode	Laboratory	Reference
$^{267}110$	$^{209}\text{Bi}(^{59}\text{Co},n)$	α decay	LBNL	[1]
$^{269}110$	$^{208}\text{Pb}(^{62}\text{Ni},n)$	α decay	GSI	[2,3]
$^{270}110$	$^{207}\text{Pb}(^{64}\text{Ni},n)$	α decay	GSI	[4]
$^{271}110$	$^{208}\text{Pb}(^{64}\text{Ni},n)$	α decay	GSI	[5]
$^{273}110$	$^{277}112$ α decay	α decay	GSI	[3,6]
	$^{244}\text{Pu}(^{34}\text{S},5n)$	α decay	JINR	[7]
$^{280}110$	$^{284}112$ α decay	fission	JINR	[8]
$^{281}110$	$^{285}112$ α decay	α decay	JINR	[9]

*Present address: National Superconducting Cyclotron Laboratory, Michigan State University, East Lansing, Michigan 48824

TABLE II. Summary of the experiment.

E_{lab} (^{64}Ni) at center of target (MeV)	Target thickness ($\mu\text{g}/\text{cm}^2$)	Dose ($\times 10^{17}$)	Decay chains observed
306.7	500	2.7	0
309.2	500	2.7	2
312.8	310	1.1	0

300- μm thick passivated ion implanted silicon detector with an active area of 116 mm (horizontal) \times 58 mm (vertical). This detector recorded the time, energy, and position of the implanted EVR's and of their subsequent α decays. It featured 32 independent vertical strips providing a 3.6-mm horizontal position accuracy. Resistive charge division provided vertical position resolution within each strip. We calibrated the energy response of each strip of the detector using the α decay of the following implanted atoms: $^{99}\text{Po}^m$ (6.059 MeV), ^{208}Po (5.115 MeV), ^{210}Po (5.3044 MeV), ^{211}Po (7.451 MeV), and ^{211}At (5.868 MeV); the strip detector had an average energy resolution of 70 keV for (5–9)-MeV α particles. The detector's geometrical efficiency for recording the full energy of an α particle from the single decay of an implanted ion was 50%; this value results in an 81% efficiency for observing at least two full-energy events of a five-member α -decay chain.

A 10-cm \times 10-cm parallel plate avalanche counter (PPAC) [17], placed 24 cm in front of the strip detector, recorded the time and position of recoiling ions before implantation. The presence or absence of signals from ions passing through the PPAC distinguished beam-related events in the strip detector and those from the α decay of previously implanted ions. The average total counting rate ($E \geq 0.5$ MeV) over the entire strip detector (after applying the PPAC veto) was observed to be $\sim 1.3/\text{s}$.

The primary difference in the LBNL measurement compared to the one at the GSI was the use of a gas-filled separator to enhance the collection of EVR's produced in the reaction. The efficiency of the setup for transport and implantation of EVR's from the $^{64}\text{Ni} + ^{208}\text{Pb}$ reaction was estimated to be 70% based on a Monte Carlo simulation [18].

TABLE III. Summary of the two element 110 decay chains. The notation “(esc)” marks decay events in which the α particle presumably escaped from the beam-facing surface of the strip detector and, thus, deposited only part of its energy to be recorded.

Interpretation	Strip-27 decay chain		Strip-19 decay chain	
	E (MeV)	Δt (s)	E (MeV)	Δt (s)
EVR implantation	20.5		18.7	
$^{271}\text{110}$ decay	10.72	0.002828	0.90 (esc)	0.001191
^{267}Hs decay	9.89	0.015320	9.88	0.032094
^{263}Sg decay	9.24	0.400610	0.65 (esc)	0.239744
^{259}Rf decay	2.45 (esc)	10.510154	2.13 (esc)	1.027344
^{255}No decay			7.81	172.619659

The assumptions in the simulation included: a Gaussian beam energy distribution, a Gaussian beam angle distribution defined by beamline limits, a linear beam energy loss in the target, and a 5-MeV (lab frame) FWHM Gaussian excitation function centered at the central thickness of the target. The simulation includes: the effect of the EVR velocity spread from the evaporation of the neutron, scattering and energy loss of the EVR in the remaining target material, and charge exchange, scattering, and energy loss in the BGS helium.

We employed three nonrestrictive strategies to search for possible chains of correlated events. We searched for: (1) pairs of decay events with energies matching those previously observed for $^{271}\text{110}$, ^{267}Hs , ^{263}Sg , ^{259}Rf , and ^{255}No anywhere within a strip and within appropriate time windows, (2) recoil events which were followed by decay events with energies matching those previously observed for $^{271}\text{110}$, ^{267}Hs , or ^{263}Sg anywhere within the same strip and within appropriate time windows, (3) recoil events which were followed by any three decay events with energies above 0.5 MeV anywhere within the same strip and within a 0.5 second time window.

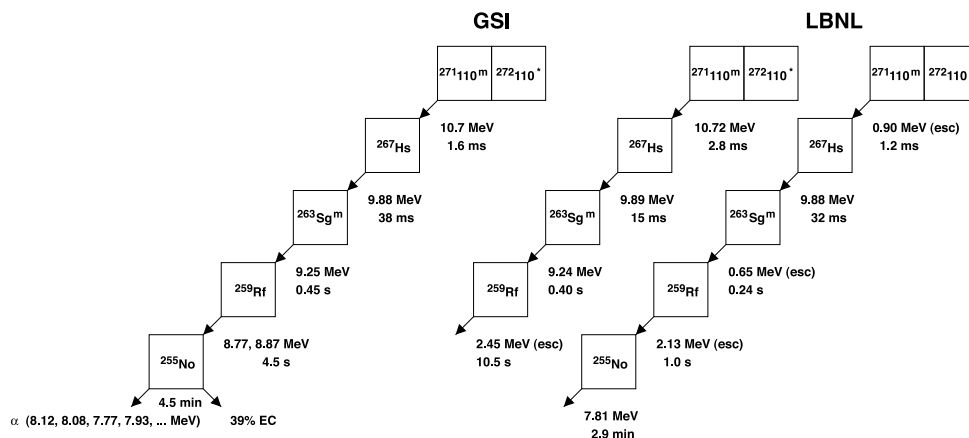


FIG. 1. Comparison of the known [5] decay sequence for $^{271}\text{110}$ (as summarized in Ref. [10]) with the two decay chains observed in this work.

TABLE IV. A listing of the $^{271}110$ decay sequences observed at the GSI [18] and the LBNL. Each row lists the α -decay energies observed in a single chain. Values in parentheses indicate α particles that “escaped” from the detector and hence did not deposit their full energy.

Laboratory	Year	Observed α -decay energies (MeV)				
		$^{271}110$	^{267}Hs	^{263}Sg	^{259}Rf	^{255}No
GSI	1994	10.68	9.89	9.25	(2.26)	
GSI	1994	10.73	(2.92)	9.24	8.86	
GSI	1994	10.73	(2.26)	(1.78)	8.90	
GSI	1994	10.73	9.87	9.23	8.79	
GSI	1994	10.71	9.83	9.24	8.75	
GSI	1994	(5.29)	9.89	9.26	8.89	8.30
GSI	1994	10.75	9.75	9.24		
GSI	1994	10.75	9.88	9.26	8.88	7.93
GSI	1994	10.74	9.88	9.25	8.74	8.09
GSI	2000	10.75	9.89	9.19	8.92	8.15
GSI	2000	10.75	9.88	9.26	8.90	
GSI	2000	10.77	(2.07)	9.06	8.77	
GSI	2000	10.82	9.88	(1.39)	8.89	8.30
LBNL	2000	10.72	9.89	9.24	(2.45)	
LBNL	2000	(0.90)	9.88	(0.65)	(2.13)	7.81

At the 315-MeV beam energy ($E_{center\ of\ target} = 309.2$ MeV), we observed two chains of events, correlated in position and time, which we interpret as the synthesis and decay of $^{271}110$. At the other two beam energies, we observed no correlated event sequences arising from $^{271}110$. A summary of the experiment is given in Table II.

Table III lists the two chains and details their physical interpretation. In the first sequence, which occurred in strip 27, all the events clustered within a narrowly defined vertical position in the strip. In the second sequence, which took place in strip 19, the EVR event and the decay events at 9.88 MeV and 7.81 MeV also occurred within a narrowly defined vertical position. The fact that these strip-19 events took place at the other end of the strip from the one used to measure the position signals is consistent with the fact that no position data are available for the remaining decay events. The small signals from these low-energy escape events were below the threshold setting for the position ADC. No other strip-19 events occurred at times between those at 18.7, 0.90, 9.88, 0.65, and 2.13 MeV.

The final member of the decay chain, ^{255}No ($t_{1/2} = 3.1$ min), decays either to ^{251}Fm ($t_{1/2} = 5.3$ h) or to ^{255}Md ($t_{1/2} = 27$ min, 92% EC decay to $t_{1/2} = 20.1$ h ^{255}Fm); both of these branches are beyond the sensitivity of the experiment. The PPAC, which has a carbon-equivalent thickness of 0.6 mg/cm², lowers the energy of the EVR’s from 70 MeV to ~ 30 MeV; a pulse-height-defect of 50%, typical for very heavy ions [19], helps to explain the observed EVR energies of ~ 20 MeV.

Figure 1 compares these decay sequences to the known decay data for $^{271}110$. Table IV shows the two $^{271}110$ decay chains reported here listed together with those reported from the GSI [20]. The agreement between our observations and the previous work is striking.

We now present an argument to show the improbability that these events arise from accidental coincidences. The second and the fourth columns of Table V list the observed implantation events in strips 19 and 27, respectively, grouped according to the number of decay events observed in the 50 s time window following each implantation. (This table does not include recoil or decay events with energies below 0.5 MeV.) Assuming that these distributions originated from random coincidences, they will be governed by the Poisson statistics

$$P(n, \mu) = \frac{\mu^n}{n!} e^{-\mu}, \quad n = 0, 1, 2, \dots, \quad (1)$$

TABLE V. Observed implantation events for strips 19 and 27, grouped according to the number of decay events n that follow within a 50 s time window. The observed distribution is compared to the expected distribution, as calculated on the basis of the simple Poisson model discussed in the text.

n	Implant event distribution			
	Strip 19		Strip 27	
	Observed	Expected	Observed	Expected
0	8369	8369	4275	4275
1	7815	7853	5576	5770
2	3651	3684	3863	3894
3	1202	1152	1783	1752
4	280	270	707	591
5	57	51	212	160
6	12	8	56	36
7	2	1	10	7
8	0	0.1	3	1
9	0	0.01	0	0.2

TABLE VI. The same data as in Table V, except grouped according to the number of decay events n that follow within a 0.5 s time window. The entries corresponding to the two 110 chains are listed in bold.

n	Implant event distribution			
	Strip 19		Strip 27	
	Observed	Expected	Observed	Expected
0	21179	21179	16242	16242
1	209	209	241	241
2	0	1	1	2
3	1	0.003	1	0.009

where $P(n, \mu)$ is the probability of observing n -decay events following any recoil (within a specified time window) when μ are expected. The third and the fifth columns of Table V show the distribution of recoil events expected for strips 19 and 27 based on this model with μ determined in each case based on the observed number of recoil events with no decay events in the time window compared to the total number of recoil events. The consistency between the observed and expected distributions shows that we are justified in assuming a Poisson model and that the observed recoil-decay coincidences are indeed accidental.

Table VI repeats the exercise of Table V except that a 0.5 s decay time window is used to group the implantation events. The entries in bold correspond to the two observed decay chains. They clearly stand out—by more than two orders of magnitude—above the background from random correlations and, therefore, are quite unlikely to result from accidental coincidences. Note that this analysis does not make use of the requirements that (1) the energies of the events should agree with previous observations, (2) the time pattern among the events should be consistent with previous measurements, or (3) the events within each chain must have closely matching vertical positions within the strip. The addition of these three very highly selective criteria—all of which are satisfied by this data—clearly demonstrates that the two chains originate from genetically linked decay events in the detector.

The raw data containing each of the two decay chains have been subjected to close scrutiny to ensure that these events are not the result of the same process leading to the incorrect report of element 118 [21].

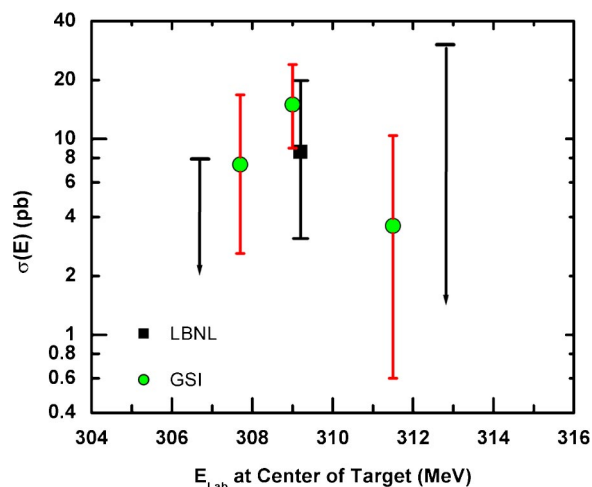


FIG. 2. (Color online) Comparison of the observed production cross sections for $^{271}\text{110}$ with those measured at the GSI [5].

The production cross section corresponding to the two $^{271}\text{110}$ decay sequences at 309.2 MeV is $8.3^{+11}_{-5.3}$ pb [22]. The “one event” upper limit cross section—i.e., the cross section obtained by assuming one event is detected when none are present—for the bombardments at 306.7 and 312.8 MeV are 7.7 and 29 pb, respectively. The cross sections were calculated assuming their values to be constant for all beam energies throughout the target thickness. Figure 2 provides a comparison between these cross sections and the previous observations at the GSI [5]; it shows an agreement within the experimental uncertainties.

In conclusion, we have confirmed the production of element $^{271}\text{110}$ in the $^{208}\text{Pb}(^{64}\text{Ni}, n)$ reaction, as reported in Ref. [5].

We acknowledge Victor Ninov for his participation in this work. We thank the operations staff of the 88-Inch Cyclotron for providing intense, steady beams of ^{64}Ni . We thank M. Steiner, J. Yurkon, and D. J. Morrissey at Michigan State University for providing the PPAC. Financial support was provided by the Office of High Energy and Nuclear Physics, Nuclear Physics Division of the U.S. Department of Energy, under Contract No. DE-AC03-76SF00098 and Grant No. DE-FG06-88ER40402.

- [1] A. Ghiorso *et al.*, Nucl. Phys. **A583**, 861c (1995); Phys. Rev. C **51**, R2293 (1995).
 [2] S. Hofmann *et al.*, Z. Phys. A **350**, 277 (1995).
 [3] S. Hofmann *et al.*, Eur. Phys. J. A **14**, 147 (2002).
 [4] S. Hofmann *et al.*, Eur. Phys. J. A **10**, 5 (2001).
 [5] S. Hofmann, Rep. Prog. Phys. **61**, 639 (1998).
 [6] S. Hofmann *et al.*, Z. Phys. A **354**, 229 (1996).
 [7] Yu.A. Lazarev *et al.*, Phys. Rev. C **54**, 620 (1996).
 [8] Yu.Ts. Oganessian *et al.*, Phys. Rev. C **62**, 041604(R) (2000);

63, 011301(R) (2001).

- [9] Yu.Ts. Oganessian *et al.*, Phys. Rev. Lett. **83**, 3154 (1999).
 [10] S. Chu, L. P. Ekstrom, and R. B. Firestone, WWW Table of Radioactive Isotopes, database version 2.0, 1999.
 [11] Yu.A. Lazarev *et al.*, Phys. Rev. Lett. **75**, 1903 (1995).
 [12] T. N. Ginter *et al.*, Proceedings of the Third International Conference on Fission and Properties of Neutron-Rich Nuclei, Sanibel Island, Florida (World Scientific, Singapore, in press).

- [13] V. Ninov, K. E. Gregorich, and C. A. McGrath, in *ENAM98*, edited by B. M. Sherrill, D. J. Morrissey, and C. N. Davids, AIP Conf. Proc. No. 455 (AIP, Woodbury, 1999), p. 704.
- [14] K. E. Gregorich *et al.*, *Eur. Phys. J. A* (in press).
- [15] F. Hubert, R. Bimbot, and H. Gauvin, *At. Data Nucl. Data Tables* **46**, 1 (1990).
- [16] A. Ghiorso *et al.*, *Nucl. Instrum. Methods Phys. Res. A* **269**, 192 (1988).
- [17] D. Swan, J. Yurkon, and D.J. Morrissey, *Nucl. Instrum. Methods Phys. Res. A* **348**, 314 (1994).
- [18] K. E. Gregorich *et al.* (unpublished).
- [19] W. Loveland, R. Yanez, K. Aleklett, J. O. Liljenzin, and A. Ghiorso, Nuclear Chemistry Progress Report, Oregon State University, 1993, p. 34.
- [20] S. Hofmann (private communication).
- [21] V. Ninov *et al.*, *Phys. Rev. Lett.* **89**, 039901(E) (2002).
- [22] K.-H. Schmidt, C.-C. Sahm, K. Pielenz, and H.-G. Clerc, *Z. Phys. A* **316**, 19 (1984).